

## Quantum vortex motion in high- $T_c$ superconductors

A. García, X. X. Zhang, and J. Tejada

*Departament de Física Fonamental, Universitat de Barcelona, Diagonal 647, E-08028 Barcelona, Spain*

Magnetic relaxation experiments at low temperatures were performed in different zero-field-cooled (ZFC) and field-cooled (FC) high- $T_c$  superconductors (HTSCs): TlBaCaCuO (2212 and 2223 phases, polycrystalline and thin-film samples), (Hg,Tl)BaCaCuO (1223 phase, polycrystalline material), and (Bi,Pb)SrCaCuO (2212 phase, single crystal). For each system and in the whole temperature range investigated, the relaxation curves obtained after both cooling processes are linear with the logarithm of time. The temperature dependence of the relaxation rate normalized to the first magnetization value,  $R = |d(M/M_0)/d \ln(t)|$ , follows a trend which is common to all systems:  $R$  decreases linearly with decreasing temperature down to a value, which is called the crossover temperature, below which it levels off to a  $T$ -independent plateau. This behavior gives evidence of a transition in the mechanism responsible for the relaxation process at low temperatures, from thermally activated (linear dependence on  $T$ ) to quantum vortex motion ( $T$ -independent regime). The experimental values for the crossover temperatures and normalized relaxation rates compare fairly well to numerical estimates in the framework of the theories of quantum vortex motion in layered HTSCs. Finally, the transition from one regime into another was studied in two samples of the TlBaCaCuO, 2223 phase, system in order to investigate the influence of dissipation on the quantum process. A clear conclusion on this point could not be drawn from these kinds of measurements. © 1996 American Institute of Physics. [S0021-8979(96)57408-0]

During recent years, quantum motion of vortices at low temperatures in high- $T_c$  superconductors (HTSCs) has been extensively investigated in a great variety of systems, mainly by means of the detection of the time evolution of the magnetization.<sup>1,2</sup> At low temperatures this decay with time, which is known as magnetic relaxation, is usually well fitted to a logarithmic law,  $M(t) = M_0[1 - R(T)\ln(t/t_0)]$ , where  $M_0$  is the first magnetization point recorded at  $t_0$  and  $R(T)$  is called the normalized relaxation rate,  $R \equiv |d \ln(M/M_0)/d \ln(t)|$ . The time-logarithmic law is the natural dependence found in the Anderson–Kim model<sup>3</sup> for thermally activated flux creep and is restricted to the low-temperature regime. As far as a linear dependence is predicted by this model,  $R$  should vanish as temperature goes to zero; however, in all reports mentioned above, as the temperature tends to zero,  $R$  presents a large, temperature-independent plateau, rather than extrapolating to zero, suggesting a decay of magnetization by quantum motion of vortices through the energy barriers.

Quantum vortex motion in HTSC was first described by Blatter and Geshkenbein in the context of the quantum collective creep (QCC) theory.<sup>4</sup> In this theory, the normalized relaxation rate at  $T=0$  in the regime of single vortex pinning is given by  $R \approx -\hbar/S_E^{\text{eff}}$ , where  $S_E^{\text{eff}}$  is the saddle-point solution for the effective Euclidean action of the tunneling process in the limit of strong ohmic dissipation, and is given by the following expressions:<sup>5</sup>

$$S_E^{\text{eff}}/\hbar \approx (\hbar/e^2)(L_c/\rho_n) \quad (3D \text{ case}), \quad (1a)$$

$$S_E^{\text{eff}}/\hbar \approx (\hbar/e^2)(d/\rho_n) \quad (2D \text{ case}). \quad (1b)$$

In these equations  $\hbar/e^2 \approx 4.1 \text{ k}\Omega$  is the quantum of resistance,  $\rho_n$  is the normal state resistivity extrapolated at  $T=0$ ,  $d$  is the interlayer spacing,  $L_c \approx (\xi/\gamma)(J_0/J_c)^{1/2}$  is the longitudinal dimension of the tunneling object,  $\xi$  is the superconducting coherence length at  $T=0$ , and  $J_0$  and  $J_c$  are the depairing and critical current density. All values are taken in the  $a$ - $b$  plane.

Because of the layered nature of HTSCs, a flux line in these materials can be pictured as a stack of two-dimensional (2D) pancake vortices lying in adjacent copper oxide layers, connected by Josephson vortices.<sup>6</sup> The dimensionality of the object involved in the tunneling process, however, depends on the strength of the magnetic field applied before or during the measurements relative to a certain dimensional crossover field,  $H_{3D-2D} \approx \Phi_0/(\gamma d)^2$ , where  $\Phi_0$  is the flux quantum, and  $\gamma$  is the anisotropy parameter of the material. Below  $H_{3D-2D}$ , 2D pancake vortices are coupled along the  $c$  axis and form a three-dimensional (3D) flux line. In this case, the Euclidean action is given by Eq. (1a) and the normalized relaxation rate is represented as  $R_{d,3D}$ , where the subscript  $d$  stands for the dissipative limit. On the other hand, for fields larger than  $H_{3D-2D}$ , the interaction within one layer is stronger than the interaction between adjacent layers, and 2D pancake vortices become decoupled. In this case, the Euclidean action is given by Eq. (1b) and the normalized relaxation rate is represented as  $R_{d,2D}$ .

Very recently, Feigel'man *et al.*<sup>7</sup> suggested that, because of the special values of their superconducting parameters, HTSCs at low temperatures should enter a nondissipative regime in which vortex motion is dominated by the Magnus instead of the friction force acting on it. In this limit, the

TABLE I. Superconducting transition temperature  $T_c$ , lower critical field  $H_{c1}$  at 5 K, dimensional crossover field  $H_{3D-2D}$  and applied magnetic field  $H_a$  for the different samples. For each  $T_c$  the magnetic field at which it has been measured is reported. In sintered samples, only intragranular  $H_{c1}$  are listed.

	Tl-pd	Tl-ps	Tl-f	Hg-ps	Bi-sc
$T_c$ (K)	108 (100 Oe)	116 (50 Oe)	112 (1 Oe)	133 (50 Oe)	85 (10 Oe)
$H_{c1}$ (kOe)	0.3	0.7	0.03	0.14	0.08
$H_{3D-2D}$ (kOe)	0.007	16	16	10	0.2
$H_a$ (kOe) for $M_{ZFC}$	1.5	...	0.5	...	0.1
$H_a$ (kOe) for $M_r$	0.1	3, 6	0.5	3, 10	...

expressions for the Euclidean action are the following:<sup>7</sup>

$$S_E^H/\hbar \approx n_s \xi^2 L_c \quad (3D \text{ case}), \quad (2a)$$

$$S_E^H/\hbar \approx n_s \xi^2 d \quad (2D \text{ case}), \quad (2b)$$

where  $n_s$  is the density of superelectrons. The corresponding normalized relaxation rates will be represented as  $R_{H,3D}$  and  $R_{H,2D}$  for the 3D and 2D cases, respectively, where the subscript  $H$  stands for the Hall limit.

The calculations so far reported correspond to the limit of zero temperature. At finite temperatures, however, quantum tunneling is thermally assisted and a gradual transition, instead of the sharp one which characterizes the  $T=0$  limit, from thermal to quantum vortex motion occurs,<sup>4</sup>

$$R(T) = R(0)[1 + (T/T_0)^2], \quad (3a)$$

$$R(T) = R(0)[1 + \exp(-T_0/T)], \quad (3b)$$

corresponding respectively to the strong-ohmic-dissipative and nondissipative limit, which includes the Hall limit. In these equations,  $T_0$  is a characteristic temperature. In any case, the quantum rate will be thermally assisted up to a crossover temperature  $T_{cr}$  which is given by<sup>4</sup>

$$\hbar/S_E^{(eff)}(0) \approx k_B T_{cr}/U_c, \quad (4)$$

where  $\hbar/S_E^{(eff)}(0)$  is the normalized relaxation rate at  $T=0$  and  $U_c$  is the energy barrier for thermal activation.

In this article we present experimental evidence of quantum vortex motion at low temperatures in different samples: polycrystalline sintered and epitaxial thin-film  $Tl_2Ba_2Ca_2Cu_3O_{10}$  (Tl-ps and Tl-f respectively), polycrystalline sintered (Hg,Tl) $Ba_2Ca_2Cu_3O_8$  (Hg-ps), polycrystalline powder  $Tl_2Ba_2CaCu_2O_8$  (Tl-pd), and single-crystal (Bi,Pb) $Sr_2CaCu_2O_8$  (Bi-sc). Details on each sample preparation are described elsewhere.<sup>8,9</sup> The magnetic relaxation measurements were performed in a commercial ac superconducting quantum interference device (SQUID) (Quantum Design) magnetometer ( $1.8 < T < 400$  K;  $H_{max} = 5.5$  T), following two different procedures. In the first one, the sample was cooled from  $T > T_c$  in a zero applied field [zero-field-cooling (ZFC) process] down to the working temperature and, after attaining a stable temperature (temperature stability was 0.01 K in the low-temperature range), a magnetic field was switched on and kept constant during the measurement of the time decay of the ZFC magnetization:  $M_{ZFC}$  vs  $t$ . In the second procedure, the sample was cooled with a mag-

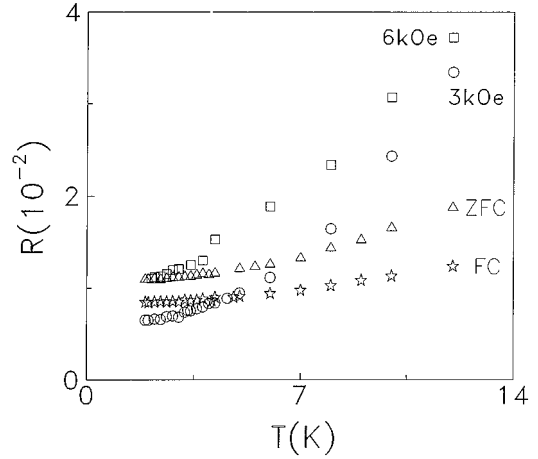


FIG. 1. Temperature dependence of the normalized relaxation rate for the Tl-ps and Tl-f samples. Circles and squares correspond to  $M_r$  of Tl-ps obtained with  $H_a = 3$  and 6 kOe, respectively; triangles and stars represent, respectively,  $M_{ZFC}$  and  $M_r$  of Tl-f obtained with  $H_a = 0.5$  kOe.

netic field applied on [field-cooling (FC) process] and, after attaining a stable temperature, the field was switched off and the remanent magnetization was recorded as a function of time:  $M_r$  vs  $t$ . After each run was complete the sample temperature was raised well above  $T_c$  in order to remove completely the trapped flux lines. Table I summarizes the superconducting transition temperature  $T_c$ , lower critical field  $H_{c1}$ , dimensional crossover field  $H_{3D-2D}$ , and magnetic procedures performed for each sample.

In the whole low-temperature range investigated ( $1.8 < T < 20$  K), the evolution with time of the remanent and ZFC magnetization of all samples is very well fitted to a time-logarithmic law in the studied time window (the total duration of each measurement was about 1 h). Figure 1 presents the temperature dependence of the normalized relaxation rates corresponding to Tl-f ( $M_{ZFC}$  and  $M_r$  obtained with 0.5 kOe) and Tl-ps ( $M_r$  obtained with  $H_a = 3$  and 6 kOe). As

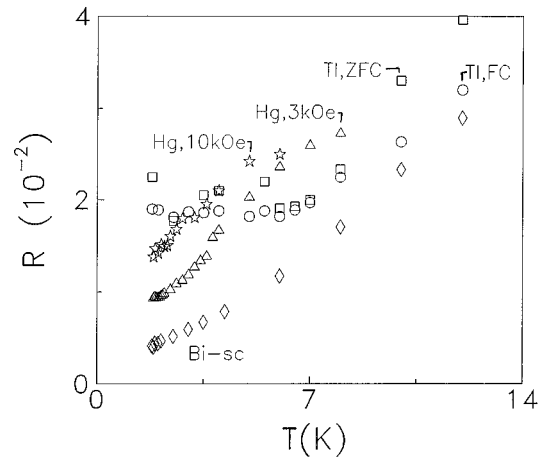


FIG. 2. Normalized relaxation rate vs temperature for Tl-pd, Hg-ps, and Bi-sc. Circles and squares stand, respectively, for Tl-pd  $M_r$  obtained with  $H_a = 0.1$  kOe and  $M_{ZFC}$  with  $H_a = 1.5$  kOe, triangles and stars represent  $M_r$  of Hg-ps obtained with  $H_a = 3$  and 10 kOe, respectively; diamonds are used for Bi-sc.

TABLE II. Experimental and estimated parameters for the samples where quantum tunneling is observed. From top to bottom: experimental value ( $R_{0,e}$ ), dissipative ( $R_d$ ), and Hall ( $R_H$ ) estimate for the plateau; experimental plateau temperature ( $T_p$ ), and estimated crossover temperature ( $T_{cr}$ ). When appropriate, the applied magnetic field or the type of magnetization is reported.

	Tl-ps	Tl-f	Tl-pd	Hg-ps
$R_{0,e}$ (%)	0.7 (3 kOe), 1.1 (6 kOe)	0.85 ( $M_r$ ), 1.1 ( $M_{ZFC}$ )	2	1 (3 kOe)
$R_d$ (%)	1.6	1.6	2.4	2.3
$R_H$ (%)	5	5	7	7
$T_p$ (K)	2.5–3	2.5–3	5–6	2.1
$T_{cr}$ (K)	4	7–8	6–7	2.6

temperature decreases, all curves show a transition from a more or less linear dependence to a temperature-independent plateau which begins between  $T_p \approx 2.5$  and 3 K, suggesting a crossover from thermal to quantum vortex motion at low temperatures. The experimental plateau values  $R_{0,e}$  are similar for both samples: For Tl-ps,  $R_{0,e} \approx 0.7\%$  for  $H_a = 3$  kOe and  $\approx 1.1\%$  for  $H_a = 6$  kOe;  $R_{0,e} \approx 0.85\%$  and  $\approx 1.1\%$  for the Tl-f FC and ZFC curves, respectively. In order to compare with theoretical values, we must first estimate the dimensional crossover field  $H_{3D-2D}$ . Using  $\gamma \approx 20$  (Ref. 10) and  $d \approx 18$  Å (Ref. 11),  $H_{3D-2D} \approx 16$  kOe is obtained, which is larger than the magnetic fields applied. Thus, quantum vortex motion is of 3D nature in both samples. Substitution of typical HTSC values [ $(J_0/J_c)^{1/2} \approx 15$ ,  $\xi \approx 30$  Å,  $\rho_n \approx 15$   $\mu\Omega$  cm,  $n_s \approx 10^{21}$  cm $^{-3}$ ] in Eqs. (1a) and (2a), gives  $R_{d,3D} \approx 1.6\%$  and  $R_{H,3D} \approx 5\%$ , which agree qualitatively well with  $R_{0,e}$  (an attempt to obtain a quantitative agreement requires the use of more accurate parameters). Finally, good fittings of each gradual transition to Eqs. (3a) and (3b) were obtained, with comparable accuracy in both cases. Therefore, no conclusion can be drawn about the dissipative nature of the quantum process. The temperature up to which each fitting rule varies from 6 to 9 K, depending on the sample and extent of the low-temperature range studied. The crossover temperatures calculated from Eq. (4) are  $T_{cr} \approx 4$  K for Tl-ps (with  $U_c \approx 400$  K, as estimated in the thermally activated regime), and  $\approx 7$ –8 K for Tl-f (with  $U_c \approx 700$ –1000 K). Both values are larger than, but comparable in order of magnitude to,  $T_p$ .

The temperature dependence of the normalized relaxation rates corresponding to Tl-pd ( $M_r$  obtained with 0.1 kOe and  $M_{ZFC}$  obtained with 1.5 kOe), Hg-ps ( $M_r$  obtained with 3 and 10 kOe), and Bi-sc ( $M_{ZFC}$  obtained with 0.1 kOe) are plotted in Fig. 2. The transition in the Hg-ps curve for  $H_a = 3$  kOe and both two Tl-pd curves appear to be very sharp, with no evidence of thermally assisted quantum tunneling. The experimental plateau values are  $R_{0,e} \approx 1\%$  for Hg-ps and  $\approx 2\%$  for both two Tl-pd curves. Using  $\gamma \approx 30$  and  $d \approx 16$  Å for Hg-ps,<sup>9</sup> and  $\gamma \approx 350$  (Ref. 12) and  $d \approx 15$  Å (Ref. 11) for Tl-pd,  $H_{3D-2D} \approx 10$  and 0.07 kOe are, respectively, obtained. Therefore, Hg-ps is in the 3D quantum creep regime ( $H_a < H_{3D-2D}$ ), and Tl-pd is in the 2D regime ( $H_a > H_{3D-2D}$ ). Then,  $R_{d,3D} \approx 2.3\%$  and  $R_{H,3D} \approx 7\%$  are obtained for Hg-ps, while Eqs. (1b) and (2b) give  $R_{d,2D} \approx 2.4\%$  and  $R_{H,2D} \approx 7\%$  for Tl-pd, which are qualitatively comparable to  $R_{0,e}$ . The plateau temperatures are  $T_p \approx 2.1$  and  $\approx 6$  K for Hg-ps and Tl-pd, respectively, in good agreement with estimates of the crossover temperature from Eq. (4),  $T_{cr} \approx 2.6$  K for Hg-ps,

and  $\approx 6$ –7 K for Tl-pd. Finally, no plateau can be found in the Hg-ps curve with  $H_a = 10$  kOe and Bi-sc curve, suggesting that one must go down to temperatures below 1.8 K to find quantum vortex motion with these magnetic fields. Actually, very low-temperature studies in 2212 Bi-based single crystals present plateaus which begin below 2 K and stretch down to the mK regime.<sup>2</sup> Table II summarizes the relevant parameters for the samples in which quantum motion has been detected.

In summary, we have reported on the detection of quantum relaxation at low temperatures in different HTSCs. In some samples (Tl-pd, Hg-ps) the transition from the thermal to the quantum regime appears to be very sharp, while in some others (Tl-ps, Tl-f) it is more gradual. In the second case, the transition was investigated in order to gain insight on the dissipative nature of the quantum process, but no conclusion could be drawn from the present study. Finally, quantum vortex motion was not detected in a couple of samples (Hg-ps and Bi-sc), suggesting the extension of magnetic relaxation measurements to the regime of ultralow temperatures.

A.G. thanks the Generalitat de Catalunya for a Ph.D. research grant. J.T. acknowledges financial support from the European Community. X.X.Z. thanks the Universitat de Barcelona for financial support.

- <sup>1</sup>S. Uji, H. Aoki, S. Takebayashi, M. Tanaka, and M. Hashimoto, *Physica C* **207**, 112 (1993); S. Moehlecke and Y. Kopelevich, *ibid.* **222**, 149 (1994).
- <sup>2</sup>K. Aupke, T. Teruzzi, P. Visani, A. Amann, A. C. Mota, and V. N. Zavaritsky, *Physica C* **209**, 255 (1993); D. Prost, L. Fruchter, I. A. Campbell, N. Motohira, and M. Konczykowski, *Phys. Rev. B* **47**, 3457 (1993).
- <sup>3</sup>P. W. Anderson and Y. B. Kim, *Rev. Mod. Phys.* **36**, 39 (1964).
- <sup>4</sup>G. Blatter and V. B. Geshkenbein, *Phys. Rev. B* **47**, 2725 (1993).
- <sup>5</sup>G. Blatter, M. V. Feigel'man, V. B. Geshkenbein, A. I. Larkin, and V. M. Vinokur, *Rev. Mod. Phys.* **66**, 1125 (1994).
- <sup>6</sup>J. R. Clem, *Phys. Rev. B* **43**, 7837 (1991).
- <sup>7</sup>M. V. Feigel'man, V. B. Geshkenbein, A. I. Larkin, and S. Levit, *Pis'ma Zh. Eks. Teor. Fiz.* **57**, 699 (1993) [*Sov. Phys. JETP Lett.* **57**, 711 (1993)].
- <sup>8</sup>A. García, X. X. Zhang, A. M. Testa, D. Fiorani, and J. Tejada, *J. Phys. Condens. Matter* **4**, 10 341 (1992); X. X. Zhang, A. García, J. Tejada, Y. Xin, and K. W. Wong, *Physica C* **232**, 99 (1994); A. García, X. X. Zhang, J. Tejada, M. Manzel, and H. Bruchlos, *Phys. Rev. B* **50**, 9439 (1994).
- <sup>9</sup>X. X. Zhang, A. García, J. Tejada, Y. Xin, G. F. Sun, and K. W. Wong, *Phys. Rev. B* **52**, 1325 (1995).
- <sup>10</sup>O. Laborde, P. Monceau, M. Potel, J. Padiou, P. Gougeon, J. C. Levet, and H. Noel, *Physica C* **162-164**, 1619 (1989).
- <sup>11</sup>R. M. Hazen, L. W. Finger, R. J. Angel, C. T. Prewitt, N. L. Ross, C. G. Hadjidakos, P. J. Heaney, D. R. Veblen, Z. Z. Sheng, A. El Ali, and A. M. Hermann, *Phys. Rev. Lett.* **60**, 1657 (1988).
- <sup>12</sup>D. E. Farrell, R. G. Beck, M. F. Booth, C. J. Allen, E. D. Bukowski, and D. M. Ginsberg, *Phys. Rev. B* **42**, 6758 (1990).